A Section 508–conformant HTML version of this article is available at https://doi.org/10.1289/EHP806.

Effects of Inorganic Arsenic, Methylated Arsenicals, and Arsenobetaine on Atherosclerosis in the apoE$^{-/-}$ Mouse Model and the Role of As3mt-Mediated Methylation

Luis Fernando Negro Silva,[1,2] Maryse Lemaire,[1,3] Catherine A. Lemarié,[1,4] Dany Plourde,[1] Alicia M. Bolt,[1,3] Christopher Chiavatti,[1,2] D. Scott Bohle,[5] Vesna Slavkovich,[6] Joseph H. Graziano,[6] Stéphanie Lehoux,[1,2,4] and Koren K. Mann[1,2,3]

[1]Lady Davis Institute for Medical Research
[2]Division of Experimental Medicine
[3]Department of Oncology
[4]Department of Medicine, and
[5]Department of Chemistry, McGill University, Montréal, Québec, Canada
[6]Mailman School of Public Health, Columbia University, New York, New York, USA

Background: Arsenic is metabolized through a series of oxidative methylation reactions by arsenic (3) methyltransferase (As3MT) to yield methylated intermediates. Although arsenic exposure is known to increase the risk of atherosclerosis, the contribution of arsenic methylation and As3MT remains undefined.

Objectives: Our objective was to define whether methylated arsenic intermediates were proatherogenic and whether arsenic biotransformation by As3MT was required for arsenic-enhanced atherosclerosis.

Methods: We utilized the apoE$^{-/-}$ mouse model to compare atherosclerotic plaque size and composition after inorganic arsenic, methylated arsenical, or arsenobetaine exposure in drinking water. We also generated *apoE*$^{-/-}$/A*s3mt*$^{-/-}$ double knockout mice to test whether As3MT-mediated biotransformation was required for the proatherogenic effects of inorganic arsenite. Furthermore, As3MT expression and function were assessed in *in vitro* cultures of plaque-resident cells. Finally, bone marrow transplantation studies were performed to define the contribution of As3MT-mediated methylation in different cell types to the development of atherosclerosis after inorganic arsenic exposure.

Results: We found that methylated arsenicals, but not arsenobetaine, are proatherogenic and that As3MT is required for arsenic to induce reactive oxygen species and promote atherosclerosis. Importantly, As3MT was expressed and functional in multiple plaque-resident cell types, and transplant studies indicated that As3MT is required in extrahepatic tissues to promote atherosclerosis.

Conclusion: Taken together, our findings indicate that As3MT acts to promote cardiovascular toxicity of arsenic and suggest that human *AS3MT* SNPs that correlate with enzyme function could predict those most at risk to develop atherosclerosis among the millions that are exposed to arsenic. https://doi.org/10.1289/EHP806

Introduction

Arsenic exposure in humans is recognized as a major public health issue [Agency for Toxic Substances and Disease Registry (ATSDR) 2013; World Health Organization (WHO) 2001), where tens of millions of people worldwide are exposed at concentrations above maximum contaminant levels (Nordstrom 2002). Chronic exposure through drinking water increases the mortality rate (Argos et al. 2010) owing to the increased incidence of several cancers (Ahsan et al. 2007) (Smith et al. 2012; Tokar et al. 2011), cardiovascular disease (Moon et al. 2013), impairment of lung (Josyula et al. 2006) (Argos et al. 2014) and liver (Mazumder 2005) function, defective immune responses (Andrew et al. 2008; Dangleben et al. 2013), and diabetes (Navas-Acien et al. 2008). Of particular concern is the link between arsenic exposure and atherosclerosis. In fact, people exposed to even low concentrations of arsenic are at risk of developing atherosclerosis (Moon et al. 2013).

Arsenic is biotransformed through a series of oxidation and methylation reactions primarily catalyzed by arsenic (3) methyltransferase (As3MT) (Thomas et al. 2007). *As3MT* is conserved from bacteria to mammals (Thomas et al. 2007). Thus, humans are exposed to methylated intermediates generated by bacteria found in the environment (Oremland and Stolz 2003). The methylation reaction uses *S*-adenosyl-L-methionine (SAM) as the methyl donor and produces intermediate compounds that include both monomethylated (MMA V and MMA III) and dimethylated (DMA V and DMA III) forms of arsenate and arsenite. Several different molecular mechanisms have been proposed for the reaction, some involving glutathionylated-arsenic intermediates (Challenger 1947; Dheeman et al. 2014; Hayakawa et al. 2005). Regardless of the exact reaction, there is a consensus regarding the importance of the As3MT enzyme in arsenic methylation. *As3mt* knockout mice have altered retention and distribution of arsenic, with significantly decreased production of methylated intermediates (Drobna et al. 2009). Historically, this reaction was considered a detoxification process; however, it is now recognized that some intermediate species are more toxic than inorganic arsenic (Stýblo et al. 2002). Nevertheless, the relative contribution of each intermediate arsenical to specific outcomes has not been defined.

The capacity to methylate arsenic has been epidemiologically linked to cardiovascular diseases. Lower methylation capacity, indicated by higher urinary MMA% or lower urinary DMA%, was associated with increased risk of fatal and nonfatal cardiovascular disease, including atherosclerosis (Chen et al. 2013b). The same group reported a linear dose–response relationship between urinary MMA% and carotid intima media thickness (cIMT), a surrogate measure of atherosclerosis, and they proposed that incomplete methylation influences atherosclerosis

Correspondence: K.K. Mann, Lady Davis Institute for Medical Research, McGill University, 3755 Cote Ste Catherine Rd., Montreal, QC, H3T 1E2 Canada; Telephone: (514) 340-8222 ext. 2760; Email: koren.mann@mcgill.ca

Supplemental Material is available online (https://doi.org/10.1289/EHP806).

The authors declare they have no actual or potential competing financial interests.

Received 15 July 2016; Revised 21 December 2016; Accepted 21 December 2016; Published 5 July 2017.

(Chen et al. 2013a). Importantly, human *AS3MT* polymorphisms were linked to differential arsenic methylation efficacy (Engström et al. 2011). An interaction between several *AS3MT* single nucleotide polymorphisms (SNPs), arsenic content in well-drinking water, and cIMT has been reported (Wu et al. 2014), although it was not statistically significant after adjusting for multiple comparisons. These data are suggestive that certain populations may be at greater risk for cardiovascular consequences of arsenic exposure.

We utilized the apoE$^{-/-}$ mouse model to address the role of arsenic biomethylation in arsenic-induced atherosclerosis. Previously, we observed increased atherosclerotic plaque formation in the apoE$^{-/-}$ mouse model after exposure to 200 ppb (parts per billion; micrograms/liter) inorganic sodium arsenite, an environmentally relevant concentration (Lemaire et al. 2011). Here, we provide data that methylated arsenicals are also proatherogenic. Importantly, we show that As3MT expression is required for arsenic-induced atherosclerosis.

Methods

Mice

B6.129P2-*apoE*^{tm1Unc}/J (apoE$^{-/-}$) male mice were obtained from Jackson laboratory. *As3mt*$^{-/-}$ mice (C57BL/6 background) were kindly provided by D. Thomas (U.S. Environmental Protection Agency, Research Triangle Park, NC, USA). *apoE*$^{-/-}$ *As3mt*$^{-/-}$ double knockout (DKO) mice were created in our facility. All experiments were performed with male mice randomly selected from different litters. Purchased mice were acclimatized to housing conditions under a 12-h light/12-h dark cycle for at least 2 wk before experiments. All mice were fed *ad libitum*. The experimental protocol was approved by the McGill Animal Care Committee, and animals were handled in accordance with institutional guidelines. The McGill Animal Care Committee is certified by the Canadian Council on Animal Care. All animals were treated humanely and with regard for alleviation of suffering.

Exposure Protocol

Four-week-old apoE$^{-/-}$ or DKO mice were maintained for 13 wk on tap water or on tap water containing 200 ppb *m*-sodium arsenite (0.35 mg/L $NaAsO_2$; Sigma-Aldrich), disodium methyl arsonate hexahydrate DSMA (MMA V; 0.78 mg/L; Chem Service), monomethyl arsenous acid (MMA III; 0.37 mg/L) synthesized as described (Gu 2014) or cacodylic acid (DMA V; 0.43 mg/L; Sigma-Aldrich). Solutions containing arsenic were refreshed every 2 – 3 days to minimize oxidation. The mice were fed with AIN-76A purified diet containing 5% fat (by weight) with no cholesterol for all of the experiments (Harlan Laboratories Inc.), with the exception of one group of DKO mice fed with a high-fat diet (20% cocoa butter, 0.5% cholesterol, Harlan Laboratories Inc.).

Bone Marrow Transplantations

Recipient apoE$^{-/-}$ or DKO male mice were lethally irradiated (10 Gy) at 5 wk of age and were injected with donor bone marrow cells 24 h after irradiation. Donors were euthanized, and tibias and femurs were flushed with phosphate-buffered saline (PBS). The suspension was passed ≥5 times through an 18–gauge needle, then through a cell strainer (70 μm) placed into a 50–mL tube, and centrifuged at $210 \times g$ for 3 min. The cell pellet was resuspended at a density of 2.5×10^7 cells/ml, and 200 μl per mouse was injected via the tail vein. After a 4-wk recovery period, the animals were exposed to tap water or to tap water containing 200 ppb $NaAsO_2$. One group of apoE$^{-/-}$ reconstituted with DKO bone marrow was fed a high-fat diet.

Plasma Analyses

Blood (0.6 mL) was obtained by cardiac puncture, and plasma was isolated using collection tubes (EDTA BD Vacutainer SST; Becton Dickinson). Cholesterol, high- and low-density lipoproteins (HDL and LDL, respectively), triglycerides, and liver enzymes [aspartate aminotransferase (AST) and alanine aminotransferase (ALT)] were assessed by the Animal Resources Centre (McGill University, Montréal, Quebec, Canada).

Atherosclerotic Lesion Characterization

Characterization of the atherosclerotic lesions was performed as previously described (Lemaire et al. 2011). Briefly, the fixed aorta was rinsed with ultrapure water, then cut longitudinally and stained *en face* with Oil Red O (Electronic Microscopy Sciences). Images were acquired using INFINITY CAPTURE software and camera (Lumenera). Percentage of lesion area of the aortic arch, defined as the region from the first intercostal arteries to the ascending arch, was evaluated using ImageJ software [National Institutes of Health (NIH)]. The atherosclerotic lesions were also evaluated within the aortic sinus from ≥5 animals. Rinsed, fixed, and embedded frozen hearts were processed as previously described (Lemaire et al. 2011). Consecutive 6-μm cryosections were sliced from the aortic base throughout the aortic sinus, where 3–5 valve sections per animal were stained with Oil Red O to visualize the plaque areas and were analyzed for their lipid content. Aortic valves were also stained and analyzed for their collagen content (type I and type III) using picrosirius red (Polysciences) (Lemaire et al. 2011).

In Situ *Immunofluorescence*

Smooth muscle cell (SMC) and macrophage contents were assessed within the entire plaque area as previously described (Lemaire et al. 2011). Briefly, aortic sinus sections were rinsed and blocked with 3% bovine albumin serum (Sigma-Aldrich), incubated with primary antibody [1:200 for monoclonal anti-α-smooth muscle cell actin [clone 1A4], 1:50 for MOMA-2 (Abcam)], rinsed, and incubated with fluorescently labeled secondary antibodies (1:500; Invitrogen). The presence of the immunofluorescent marker from at least 3 sections per animal was quantified using ImageJ software (NIH) and was expressed as a percentage of the total lesion area.

In Situ *Dihydroethidium Staining*

Frozen aortic sinus sections were stained with 2 μM dihydroethidium (DHE) (ThermoFisher Scientific) in PBS and were analyzed immediately using a fluorescence microscope. The presence of the fluorescent marker from ≥5 sections per animal was quantified using ImageJ software (NIH): images were batch-processed by converting to 32-bit images, the colors were inverted to adjust the thresholds on a white background, and vessel perimeters were demarcated. Intensity was assessed and expressed as percentage of the total vessel area.

Primary Bone Marrow-Derived Macrophages (BMDMs) Differentiation and Polarization

Bone marrow from apoE$^{-/-}$ or DKO mice was isolated from the femur and tibia of 10- to 12-wk-old old mice. Bones were flushed with RPMI 1,640, and a single-cell suspension was created by passing it 5 times through an 18G needle. The cell suspension was filtered and centrifuged at 1,000 rpm for 3 min. Pelleted cells

were suspended in Roswell Park Memorial Institute (RPMI) 1640 medium (Wisent, Inc) plus 10 % fetal bovne serum (FBS) (Wisent, Inc) plus penicillin/streptomycin (Wisent, Inc) and were plated to perform a monocyte-enriching adherence step for 1 h. Next, nonadherent cells were removed, fresh medium was added with 50 ng/mL of macrophage colony stimulating factor (M-CSF) (Peprotech®), and the cells were cultured for 5 d. Medium was refreshed every 2–3 d. After 5 d, cells were kept in M-CSF for M0 or were polarized toward M1 using interferon gamma (IFN-γ) or toward M2 using interleukin 4 (IL-4) (50 ng/mL IFN-γ, Peprotech®, and 10 ng/mL IL-4, Peprotech®, respectively) for an additional 48 h.

Staining for Cellular Lipid Accumulation

Unpolarized (M0) BMDMs from apoE$^{-/-}$ or DKO mice was isolated as described above and cultured on cover slips for 5 d in M-CSF with or without $NaAsO_2$. Then, cells were exposed to 2.5μM 7-ketocholesterol for a further 24 h. Next, cells were stained with Oil Red O for 40 min, counterstained with hematoxylin for 2 min, and rinsed with PBS before mounting the slides. Images were acquired using INFINITY CAPTURE software and camera (Lumenera). At least 200 macrophages in 2 different fields were counted, and the results were expressed as a percentage of Oil Red O–positive cells per total cell number.

Endothelial Cell Isolation and Culture

This protocol was adapted from a protocol described by Robins et al. (2013). Endothelial cells were isolated from lungs of 8 – 10-wk-old apoE$^{-/-}$ or DKO mice. The lungs were cut into small pieces and incubated at 37°C for 60 min in 0.1% collagenase A (Roche Diagnostics) in RPMI medium plus penicillin/streptomycin. The suspension was transferred into a 50–mL tube, passed 15 times through an 18-gauge needle, and then through a cell strainer (70 μm), and was then centrifuged at 210 × *g* for 5 min. The supernatant was removed, and the cells were plated in 75-cm^2 tissue culture flasks coated with 0.1% gelatin (Millipore) and grown for 1 wk in 50% Dulbecco's Modified Eagle Medium: Nutrient Mixture F-12 (DMEM/F12; Wisent, Inc) supplemented with 10% FBS and penicillin/streptomycin and 50% Endothelial Growth Medium SingleQuot (EGM-2 SingleQuot) medium (Lonza). Endothelial cells were selected by performing two consecutive immunoisolation steps using magnetic beads conjugated with anti–intercellular adhesion molecule 2 (anti-ICAM-2) antibody (BD Biosciences PharMingen) and were plated into 75-cm^2 tissue culture–gelatin-coated flasks. Endothelial cells were used for experiments at passage 4. Cultures were serum-starved for 24 h before experiments.

Smooth Muscle Cell Isolation and Culture

SMCs were isolated from the thoracic aorta of 8- to 10-wk-old apoE$^{-/-}$ and DKO male mice (Ray et al. 2001). After removal of the adventitia, the tunica media was digested with 3 mg collagenase (Worthington Biochemical Corporation) and 3 mg elastase (Sigma-Aldrich) for 0.5 h at 37°C. The suspension was passed ≥10 times through an 18-gauge needle, then through a cell strainer (70 μm) into a 50–mL tube and centrifuged at 836 × *g* for 2 min. The supernatant was removed, and the cells were plated into 25-cm^2 tissue culture flasks in DMEM (Wisent, Inc) supplemented with 10% FBS and penicillin/streptomycin for 2 wk. Experiments were performed at passage 3 or passage 4. Cultures were serum-starved for 24 h before experiments.

In Vitro *DHE Staining*

Primary cells were isolated and cultured as described above. Cells were stained as described elsewhere (Straub et al. 2008). Briefly, BMDMs, SMCs, or endothelial cells were stained with 5 μM DHE in media for 10 min, after which 200 ppb $NaAsO_2$, MMA III, DMA V, or DMA III was added for a further 30 min. DMA III was synthesized as described (Garnier et al. 2014) and utilized immediately. Rotenone (Sigma Aldrich) at 10μM and menadione (Sigma Aldrich) at 200μM were used as positive controls. Antioxidants (1mM Tempol or 5 mM *N*-acetylcysteine) were added for 10 min before exposure. Images were obtained immediately using a fluorescence microscope. The relative fluorescence was used to determine changes in DHE oxidation normalized to the number of cells in the field.

Gene Expression

Total RNA was isolated from BMDMs using an RNeasy kit (Qiagen). Complementary DNA (cDNA) was prepared from total RNA using the iScript cDNA synthesis kit (Bio-Rad). Gene expression was analyzed by real-time polymerase chain reaction (qPCR) using the Applied Biosystems 7500 Fast RT-PCR system and Fast SYBR Green Master Mix (Life Technologies). Experiments were performed using qPCR primers designed and purchased from Integrated DNA Technologies: m36B4 (5′TCA TCCAGCAGGTGTTTGACA3′ and 5′GGCACCGAGGCAAC AGTT3′, efficiency 98.55%, slope −3.3), As3mt (5′GAAAAC TGCCGAATTTTGGA3′ and 5′GCCGTGGAGAAAAGTCA CAT3′, efficiency 97.99%, slope −3.3). Primers were validated using standard curves over 5 logs of murine C57BL6 liver cDNA. Only primers with single peaks (and no primer dimers) in melt curves were used. Experiments were performed using three technical replicates. Data were normalized to the housekeeping gene m36B4. Fold change in gene expression was determined by the $2^{-\Delta\Delta Ct}$ method using naïve gene expression as the reference sample.

Protein Quantification and Immunoblotting

Cells were lysed using radioimmunoprecipitation assay (RIPA) buffer (50 mM Tris-HCl, pH 8.0, with 150 mM sodium chloride, 1.0% Igepal CA-630 (NP-40), 0.5% sodium deoxycholate, and 0.1% sodium dodecyl sulfate) at 4°C. After sonication (Sonic Dismembrator; Fischer Scientific) with 3 pulses at 10% for 10 s, the cell lysates were centrifuged at 15,871 × *g* for 10 min. The supernatants were collected, and protein concentrations were quantified with the Bio-Rad protein assay (Bio-Rad). Samples were boiled at 95°C, and equal amounts of protein (50 μg) were loaded on a 10% sodium dodecyl sulfate–polyacrylamide gel electrophoresis (SDS-PAGE) gel. Proteins were transferred to a nitrocellulose membrane (Bio-Rad, Mississauga, CA). Membranes were blocked for 30 min with 5% milk/Tris-buffered saline (TBS) plus 10% TWEEN 20 and probed with the primary antibody overnight at 4°C. Next, the blots were incubated with anti-rabbit antibodies (BD PharMingen) for 1 h at 20–23°C, and the signals of the target proteins were developed with chemiluminescence substrate (Amersham, GE Healthcare). GAPDH or Lamin A was used as an endogenous control to confirm equal protein loading.

Antibodies

As3MT polyclonal antibody was raised in rabbit using the following synthetic peptide (EpiCypher): [C]HGRIEKLAEAGIQ SESYDIV. The amino acid in brackets was added to improve the solubility of the peptide and for coupling. Further, the peptide was conjugated to keyhole limpet hemocyanin (Sigma-Aldrich)

and was sent to Pocono Rabbit Farm & Laboratory Inc. for antibody production. Rabbit serum was affinity-purified using an antigen column with a SulfoLink immobilization kit (Thermo Scientific). Commercial antibodies were used: rabbit anti-GAPDH (Life Science) and rabbit anti-Lamin A (Santa Cruz).

Arsenic Speciation in BMDMs

Media from BMDMs were collected after 48 h of exposure to 50ppb $NaAsO_2$. Media were diluted in 0.1 volume of 150 mM aqueous mercury chloride to displace trivalent As from protein thiols. After holding these samples on ice for one minute, they were deproteinized by mixing with one volume of 0.66 M ice-cold perchloric acid ($HClO_4$)and were centrifuged for 10 min at $1{,}503 \times g$. The supernatant was sent to Columbia University (New York) for analysis. Briefly, the supernatant was mixed with mobile-phase buffer and injected onto a high performance liquid chromatography (HPLC) column connected to an inductively coupled plasma–mass spectrometry–dynamic reaction cell (ICP-MS-DRC; Perkin-Elmer). Calibration standards of As metabolite mixtures were treated the same way to achieve the same pH and composition as the deproteinized samples.

ICP-MS-DRC was coupled to HPLC and was used as a detector for six arsenic metabolites chromatographically separated by anion exchange using a Hamilton PRP-X100 column (Hamilton Company) with 10mM ammonium nitrate/ammonium phosphate, pH 9.1, as the mobile phase. Excellent separation power by HPLC, coupled with very low detection limits of ICP-MS-DRC, allowed us to detect AsC, AsB, MMA, DMA, As^{3+} and As^{5+}, without online digestion of organic forms, with great precision down to total As concentrations of 0.1 μg/L.

Statistical Considerations

For statistical analysis, one-way analysis of variance (ANOVA) was performed and the *p*-value was evaluated with Dunnett's test or a Bonferroni post hoc test using GraphPad Instat software. A *p*-value <0.05 indicated statistical significance. The data are presented as the mean values ± the standard error of the mean (SEM)

Results

Effects of Methylated Arsenicals, Inorganic Arsenic, and Arsenobetaine on Atherosclerosis and Plaque Components in the apoE$^{-/-}$ *Mouse Model*

Moderate (200 ppb) concentrations of sodium arsenite are proatherogenic in apoE$^{-/-}$ mice, such that they increase plaque formation and alter the plaque components after 13 wk of exposure through drinking water (Lemaire et al. 2011). However, the potential effects of organic arsenicals in our system were unknown. Thus, we compared the methylated arsenicals MMA V, MMA III and DMA V with inorganic arsenic ($NaAsO_2$) by exposing apoE$^{-/-}$ mice to 200 ppb of individual arsenicals in drinking water for 13 wk. The plaque formation was accessed *en face* in the aortic arch after staining with Oil Red O. Surprisingly, when compared with the control group, exposure to all of the methylated arsenicals enhanced the size of the atherosclerotic lesions (Figure 1A). We further analyzed the plaque size and components in cross-sections of the aortic sinus. Here, although we observed increased plaque size in all groups, only $NaAsO_2$ was statistically significant (Figure 1B; $p = 0.07$ for MMA V vs. control). We previously observed that $NaAsO_2$ exposure increased lipid content within the plaques without a concomitant increase in macrophage number, suggesting that each macrophage accumulated more lipids per cell (Lemaire et al. 2011). Similar analyses for lipid content by Oil Red O staining within plaques showed that methylated arsenicals increased lipids to the same extent as $NaAsO_2$ (Figure 1C) despite no change in macrophages per plaque area as assessed by immunofluorescent staining (Figure 1D). We also evaluated collagen and SMCs, increases in which promote plaque stability (Gomez and Owens 2012; Libby et al. 2011). Collagen content was reduced in groups exposed to $NaAsO_2$ and monomethylated arsenicals (MMA V and MMA III), but not in the DMA V–exposed groups (Figure 1E). Interestingly, SMC content was decreased in all arsenic-exposed groups, reaching statistical significance only in $NaAsO_2$-exposed mice (Figure 1F).

Arsenobetaine is also an organic arsenical and is the main arsenic-containing compound found in many fish (Molin et al. 2015) (Navas-Acien et al. 2011). However, it is not biotransformed by As3MT in laboratory animals (Vahter et al. 1983). We tested whether arsenobetaine also acted as a proatherogen. Interestingly, arsenobetaine exposure did not increase plaque formation in the arch or sinus (Figure 1A and 1B). Together, these observations indicate that methylated arsenicals are proatherogenic and can cause changes in plaque components in a manner similar to that of $NaAsO_2$. Further, the lack of proatherogenic activity by arsenobetaine suggests that biotransformation by As3MT is important.

Effects of As3mt *Deletion on Arsenic-Induced Atherosclerosis*

To study the relative contribution of As3MT in arsenic-induced atherosclerosis, we developed a double knockout mouse model by crossing As3mt$^{-/-}$ mice with apoE$^{-/-}$ mice. The DKO mice were viable and were born at 1:1 a sex ratio with no difference in litter size compared with apoE$^{-/-}$ mice (see Figure S1A). We confirmed the lack of As3mt expression in liver extracts from DKO mice (with and without $NaAsO_2$ exposure) (see Figure S1B), as well as the lack of arsenic methylation, by measuring methylated intermediates in the urine (Fig. S1C). No differences were observed in the body weight (see Figures S1D and S1E), circulating lipid profiles, liver enzymes, or complete blood counts (see Tables S1 and S2) between the DKO mice and the apoE$^{-/-}$ mice.

We then compared apoE$^{-/-}$ and DKO mice exposed to tap water or to 200 ppb $NaAsO_2$, MMA III, or DMA V for 13 wk and measured the extent of atherosclerotic plaque. In contrast to apoE$^{-/-}$ mice, the DKO mice exposed to $NaAsO_2$ exhibited no increased plaque formation in either the aortic arch (Figure 2A) or the aortic sinus (Figure 2B) compared with tap water–exposed mice. Moreover, exposure to methylated intermediate arsenicals did not rescue the phenotype (Fig 2A and 2B). Importantly, DKO mice were specifically protected from arsenic-enhanced atherosclerosis because a high-fat diet (HFD) enhanced plaque formation in these animals (Figure 2A and 2B). Of note, in the aortic sinus, control DKO mice had slightly more plaque area than control apoE$^{-/-}$ mice ($p = 0.0813$; Figure 2B), although this finding was not observed in the aortic arch.

Next, we evaluated whether DKO mice were also protected from arsenic-induced changes in plaque composition. In apoE$^{-/-}$ mice, both inorganic and methylated arsenicals increased lipid accumulation per macrophage, with concomitant decreases in SMCs and collagen (Figure 1C-F). In contrast, the DKO mice exposed to arsenicals exhibited no decrease in the number of SMCs (Figure 2C), and only $NaAsO_2$-exposed mice exhibited reduced collagen content (Figure 2D). Surprisingly, plaques from control, unexposed DKO mice had fewer SMCs and less collagen than control apoE$^{-/-}$ mice (Figure 2C and 2D); this paralleled the small increase in lesion area observed in the aortic sinus of DKO mice.

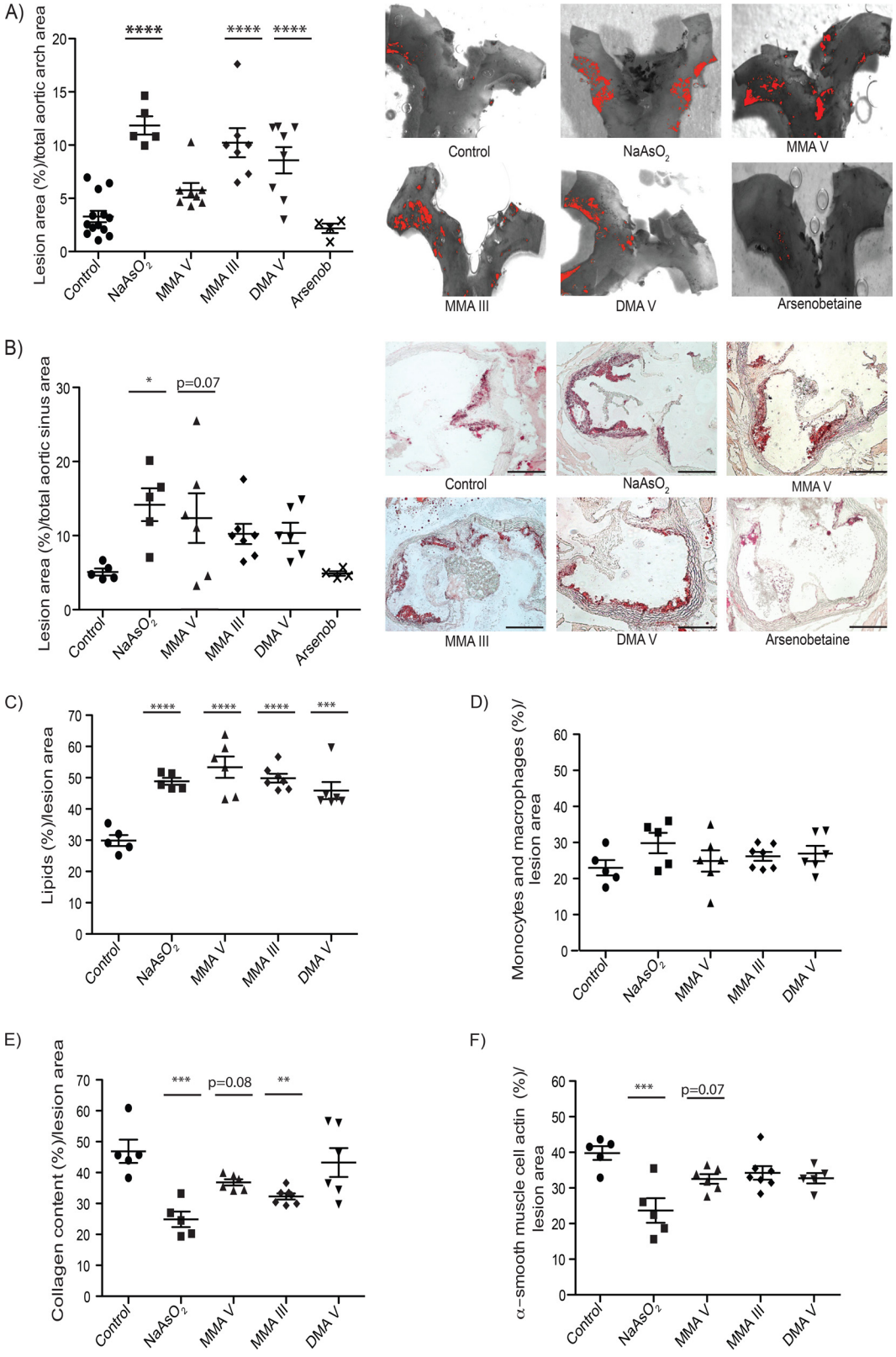

Figure 1. Effects of methylated arsenicals, inorganic arsenic, and arsenobetaine on atherosclerosis and plaque components in the apoE$^{-/-}$ mouse model. Four-week-old apoE$^{-/-}$ mice were exposed to 200 ppb arsenicals [*m*-sodium arsenite ($NaAsO_2$), monomethyl arsenic (MMA) V, MMA III, dimethyl arsenic (DMA V) or arsenobetaine (arsenob)] or maintained on tap water for 13 wk. Percent lesion area of the aortic arch (*A*) or aortic sinus (*B*) was evaluated via staining with Oil Red O. Lipid content (*C*), macrophage (*D*), collagen (*E*), and smooth muscle cell (*F*) content was evaluated in the aortic sinus relative to the total lesion area. The scale bar represents 100 µm. Values are expressed as the mean ± standard error of the mean (SEM). $*p < 0.05$; $**p < 0.01$; $***p < 0.001$; $****p < 0.0001$ relative to their own control.

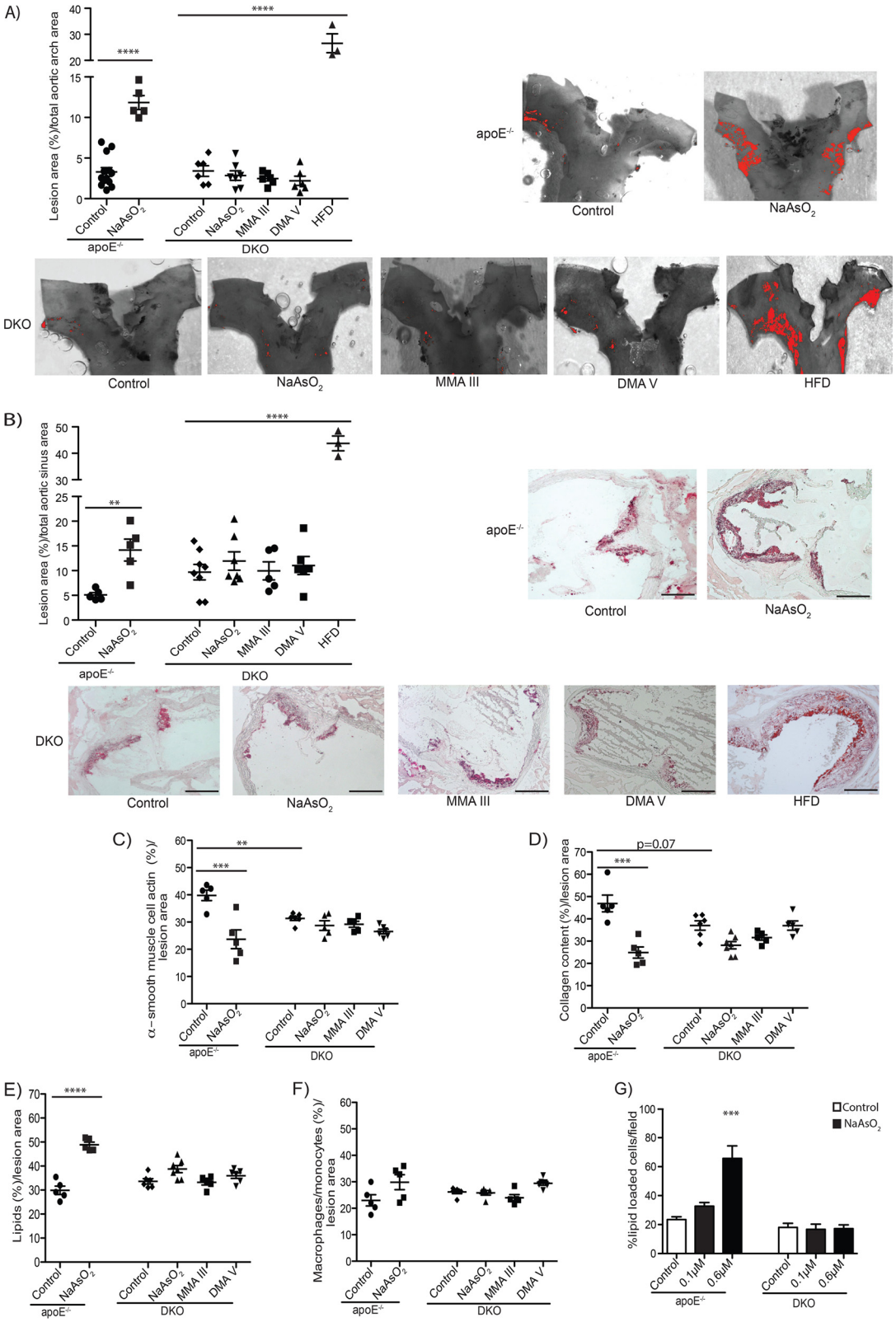

Figure 2. Effects of *As3mt* deletion on arsenic-induced atherosclerosis. Four-week-old apoE$^{-/-}$ and double knockout (DKO) mice were exposed to 200 ppb arsenicals [*m*-sodium arsenite ($NaAsO_2$, monomethyl arsenic (MMA) III or dimethyl arsenic (DMA V)] or maintained on tap water for 13 wk. An additional group of DKO mice was fed a high-fat diet (HFD) and kept on tap water. Percent lesion area of the aortic arch (*A*) or aortic sinus (*B*) was evaluated via staining with Oil Red O. Smooth muscle cell (*C*), collagen (*D*), lipid (*E*), and macrophage (*F*) content were evaluated in the aortic sinus relative to the total lesion area. Representative pictures are shown. The scale bar represents 100 μm. Bone marrow–derived macrophages from apoE$^{-/-}$ or DKO background were cultured for 5 days with or without 0.1 or 0.6 μM (10 or 50 ppb) $NaAsO_2$, after which cultures were challenged with 7-ketocholesterol for 24 h. The number of cells staining positive for lipids expressed relative to total cell amount per field was quantified (*G*). Values are expressed as the mean ± standard error of the mean (SEM). *$p < 0.05$; **$p < 0.01$; ***$p < 0.001$; ****$p < 0.0001$ relative to their own control.

Arsenical exposure did not increase lipid content (Figure 2E) or macrophage infiltration (Figure 2F) in the plaques of DKO mice. In addition, the lipid and macrophage content in plaques of unexposed DKO mice was not significantly different from that in control apoE$^{-/-}$ mice. These data suggest that As3MT is required for arsenic-induced lipid accumulation in macrophages. Considering our previous data implicating macrophage lipid homeostasis as an important target for arsenic (Lemaire et al. 2011; Lemaire et al. 2014), we further investigated the role of As3MT in arsenic-induced macrophage lipid accumulation *in vitro*. We cultured BMDMs from apoE$^{-/-}$ and DKO mice. BMDMs were exposed to 0.1 and 0.6 μM $NaAsO_2$ (corresponding to 10 and 50 ppb $NaAsO_2$) for 5 d during differentiation with M-CSF and then were challenged with 7-ketocholesterol for another 24 h. Consistent with our *in vivo* observations, $NaAsO_2$ increased the number of apoE$^{-/-}$ macrophages that stained positive for Oil Red O, indicating increased lipid accumulation in response to arsenic exposure (Figure 2G). However, the DKO BMDM were protected against arsenic-increased lipid loading (Figure 2G). These findings suggest that As3MT is required for arsenic-induced atherosclerosis. Moreover, As3MT expressed in macrophages is required for arsenic-mediated effects on lipid handling.

Effects of As3mt *Deletion on Reactive Oxygen Species Formation in* apoE$^{-/-}$ *Mice and in Primary Cells Present at the Atherosclerotic Lesion*

Increased reactive oxygen species (ROS) is a well-reported consequence of arsenic exposure (Bunderson et al. 2004; Straub et al. 2008). Furthermore, we have shown that inorganic arsenic induces ROS-mediated monocyte/endothelial cell interactions, an early event in atherosclerosis (Lemaire et al. 2015). Supplementation with the antioxidant selenium decreases arsenic-enhanced atherosclerosis (Krohn et al. 2016). Therefore, we postulated that ROS may be differentially produced between the apoE$^{-/-}$ and DKO mice following arsenical exposure. Thus, we performed DHE staining to detect ROS in aortic sinus cross-sections from apoE$^{-/-}$ and DKO mice exposed to 200 ppb arsenicals or tap water for 13 wk. All apoE$^{-/-}$ groups exposed to arsenicals had significantly increased intensity of DHE staining per vessel area when compared with controls (Figure 3A). Surprisingly, neither inorganic nor methylated arsenicals induced ROS in the absence of As3MT expression (Figure 3A). We then investigated whether specific cell types within the plaque were deficient in ROS production in the DKO mice *in vitro*. Thus, primary macrophages, SMCs, and endothelial cells were exposed to 200 ppb $NaAsO_2$ for 30 min, stained with DHE, and analyzed using a fluorescence microscope. Interestingly, macrophages (Figure 3B), endothelial cells (Figure 3C), and SMCs (Figure 3D) produced ROS in response to $NaAsO_2$ when derived from apoE$^{-/-}$ mice, but not when derived from DKO mice. Nevertheless, DKO-derived macrophages were not resistant to ROS induced by rotenone or menadione (see Figure S2A). DHE staining was reduced with antioxidants Tempol and *N*-acetylcysteine (Fig. S2B). Interestingly, the methylated arsenicals MMA III and DMA V also failed to increase ROS production in cells derived from DKO mice; however, DMA III increased ROS in both macrophages (Figure 3E) and SMCs (Figure 3F). These data indicate that As3MT expression, the methylation process, or both are required for arsenic-induced ROS in multiple cell types. Indeed, the ability of DMA III to induce ROS in DKO cells indicates that this terminal metabolite may be an important proatherogenic intermediate.

As3mt *Expression in Macrophages, SMCs and Endothelial Cells*

Clearly, *As3mt* deletion inhibits arsenic-induced ROS and atherosclerosis following exposure to either $NaAsO_2$ or methylated arsenicals. As3MT is highly expressed in the liver, but very little is known about which cell types in atherosclerotic plaque express As3MT and whether it is functional. Deletion of As3mt reduces ROS production in the aortic sinus; thus, we postulated that plaque-resident cells could express As3MT and produce methylated intermediates *in situ*.

Plaque-resident macrophages are heterogeneous and include the inflammatory M1 and alternative wound-healing M2 polarization states (Chinetti-Gbaguidi et al. 2015). Thus, we evaluated the expression of *As3MT* in BMDMs that were differentiated and polarized *in vitro*. Macrophages were cultured with classical stimuli for polarization: M0 (M-CSF), M1 (IFN-γ), and M2 (IL-4). After polarization, cells were exposed to vehicle or to 50 ppb $NaAsO_2$ for 24 h. A lower concentration of $NaAsO_2$ was chosen because differentiated macrophages are sensitive to the cytotoxic effects of 200 ppb $NaAsO_2$ at longer time points *in vitro*. As3mt mRNA was detected in all three polarized BMDMs, although at a much lower level than the expression in murine liver (Figure 4A). Next, protein expression was determined by performing Western blotting using a rabbit polyclonal antibody that we produced. As3MT protein could be detected in all macrophage subtypes (Figure 4B). In addition, As3MT protein was expressed in SMCs and in endothelial cells (Figure 4C). Notably, exposure to $NaAsO_2$ did not alter As3MT protein levels. Finally, using HPLC/ICP-MS, we determined the capacity of these cell types to methylate arsenic. Methylated forms of arsenic were detected in the media from BMDMs (Figure 4D) after arsenic exposure. Taken together, these data demonstrate that macrophages, SMCs, and endothelial cells express functional As3MT, and consequently, local arsenic methylation might be important for the pathogenesis of arsenic-induced atherosclerosis.

Effects of Bone Marrow-Derived and Non-Bone Marrow–Derived As3mt *on Arsenic-Induced Atherosclerosis*

Based on our data showing that As3MT is expressed in macrophages, endothelial cells, and SMCs, we investigated the relative contribution of bone marrow-derived versus non-bone marrow–derived As3MT on arsenic-induced atherosclerosis. We performed bone marrow transplantations in which male apoE$^{-/-}$ or DKO mice were irradiated and reconstituted with either apoE$^{-/-}$ or DKO bone marrow. After 4 wk of reconstitution, mice were maintained on tap water or were transferred to 200 ppb $NaAsO_2$ for another 13 wk. apoE$^{-/-}$ mice transplanted with apoE$^{-/-}$ bone marrow and exposed to 200 ppb $NaAsO_2$ showed increased plaque formation when compared with tap water controls (Figure 5A; see also Figure S3), which recapitulated the results that we have published previously (Lemaire et al. 2011). Furthermore, DKO mice transplanted with DKO bone marrow were protected against arsenic-induced atherosclerosis. Interestingly, neither apoE$^{-/-}$ mice transplanted with DKO bone marrow nor DKO mice reconstituted with apoE$^{-/-}$ bone marrow had increased lesion size after $NaAsO_2$ exposure compared with their respective controls (Figure 5A; see also Figure S3). We did observe that apoE$^{-/-}$ mice transplanted with DKO bone marrow had a significantly increased basal level of plaque compared with apoE$^{-/-}$ mice transplanted with apoE$^{-/-}$ bone marrow (Figure 5A and Figure S3). DKO mice reconstituted with DKO bone marrow also had slightly elevated levels of plaque size consistent with what we observed in Figure 2. Lipid (Figure 5B) and SMC (Figure 5D) content were reduced only in apoE$^{-/-}$ mice

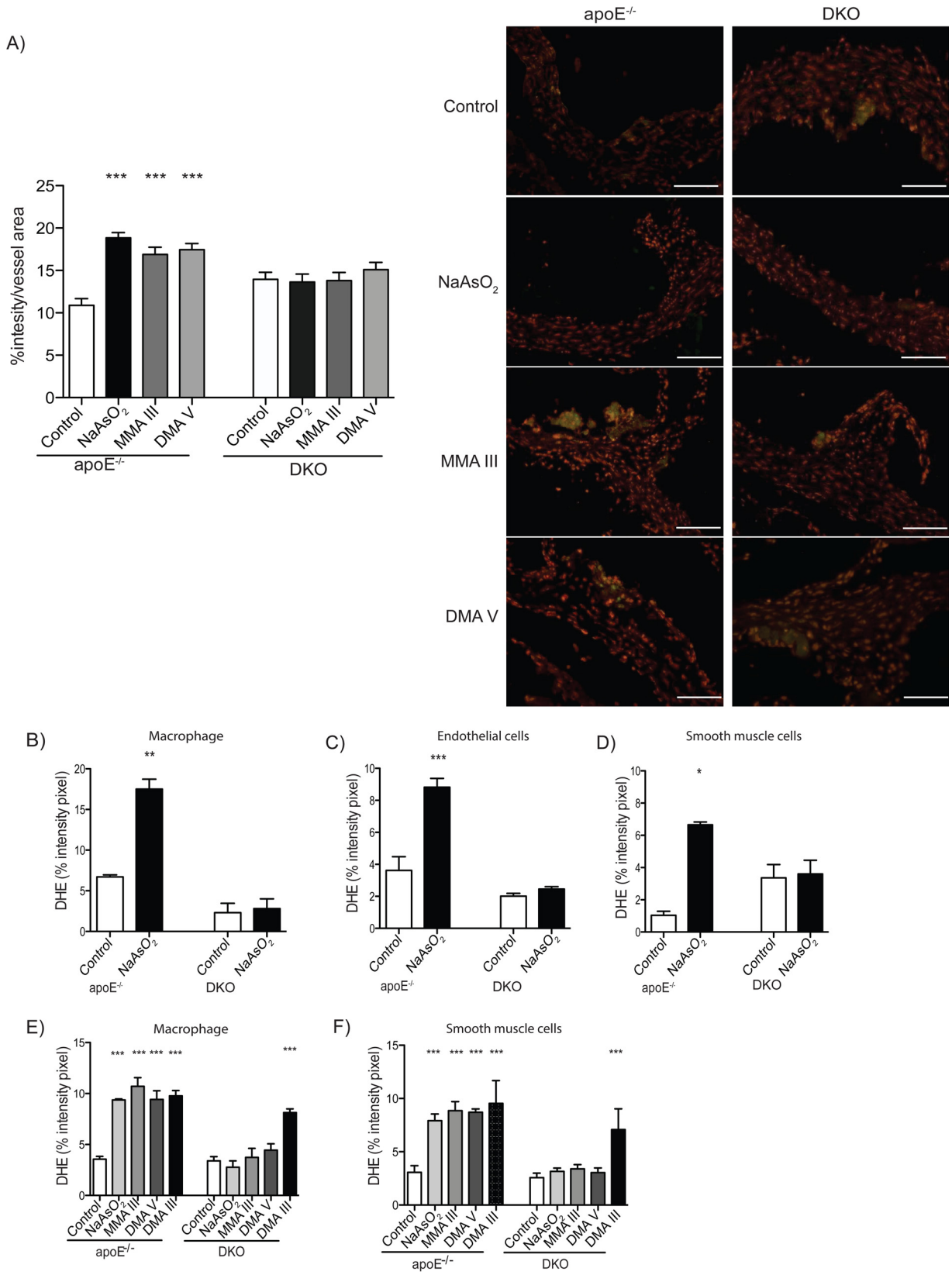

Figure 3. Effects of *As3mt* deletion on reactive oxygen species (ROS) formation in apoE$^{-/-}$ mice and in primary cells present at the atherosclerotic lesion. Four-week-old apoE$^{-/-}$ and double knockout (DKO) mice were exposed to arsenicals [*m*-sodium arsenite ($NaAsO_2$), monomethyl arsenic (MMA) V, MMA III, or dimethyl arsenic (DMA) V] at 200 ppb for 13 wk or maintained on tap water. Frozen sections (≥3 sections per animal; $n > 3$ per group) of the aortic sinus were stained with 2 μM dihydroethidium (DHE), and ROS levels were expressed as a percentage of the total vessel area (*A*). Representative pictures are shown. The scale bar represents 200μm. Bone marrow–derived macrophage (BMDM) (*B* and *E*), endothelial cells (*C*), and smooth muscle cells (*D* and *F*) derived from apoE$^{-/-}$ or DKO mice were pretreated with 5 μM DHE for 10 min, and then the cultures were exposed to 200 ppb $NaAsO_2$, MMA III, DMA V, or DMA III for another 30 min. Data are expressed as the mean ± standard error of the mean (SEM) from three independent experiments. *$p < 0.05$; **$p < 0.01$ relative to their own control.

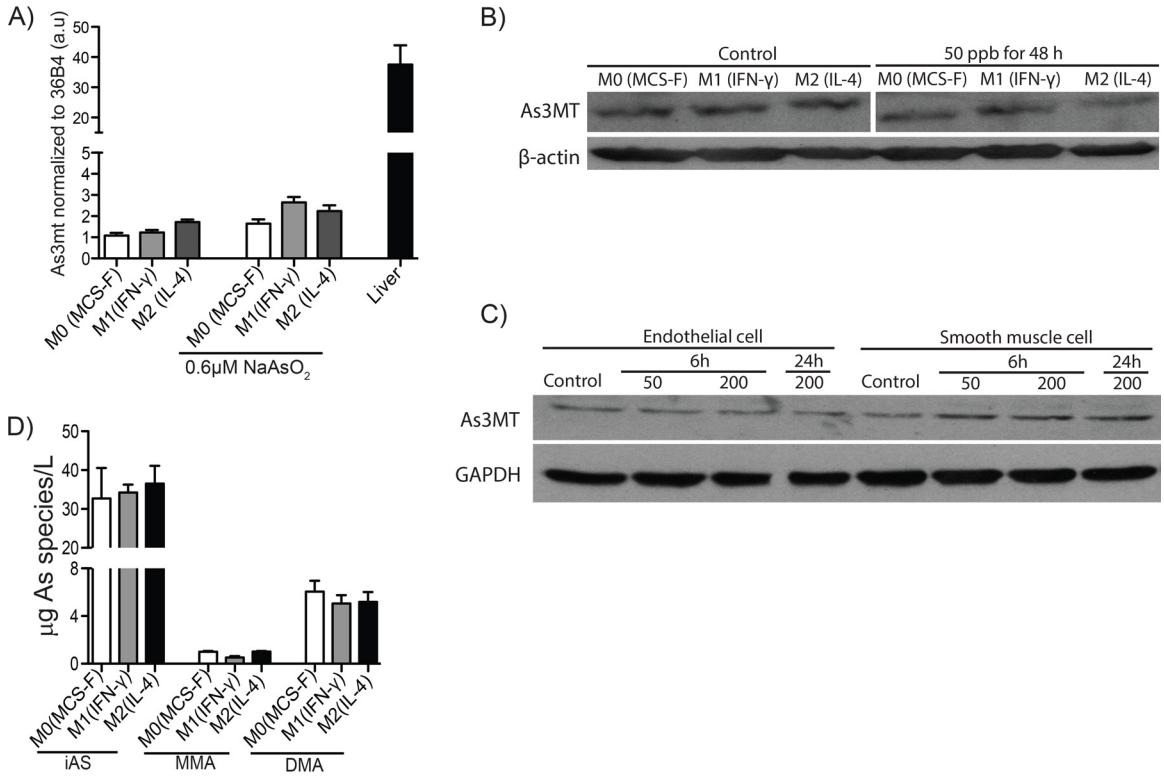

Figure 4. *As3mt* expression in macrophages, smooth muscle cells and endothelial cells. Total RNA from bone marrow–derived macrophage (BMDM) and liver from apoE$^{-/-}$ mice was isolated, and *As3mt* gene expression was assessed by real-time polymerase chain reaction (qPCR). Each sample was analyzed in triplicate (technical replicate) and expressed relative to the *m36B4* housekeeping gene (arbitrary units) (*A*). Immunoblots for As3MT were performed from whole cell extracts of BMDM (*B*), endothelial cells or smooth muscle cell (SMC) cultures (*C*) exposed to sodium arsenite ($NaAsO_2$) at the time and concentration indicated. Three independent experiments were performed. Arsenic methylation profiles in the media from BMDM (*D*) were assessed by high performance liquid chromatography–inductively coupled plasma–mass spectrometry (HPLC-ICP-MS). iAs, inorganic arsenic; MMA, monomethyl arsenic; DMA, dimethyl arsenic.

transplanted with apoE$^{-/-}$ bone marrow. Collectively, the data reveal that both host- and bone marrow-derived cells participate in arsenic methylation and are mandatory for arsenic-induced atherosclerosis.

Discussion

Epidemiologic studies have linked arsenic exposure to increased cardiovascular disease. However, the contribution of arsenic biomethylation is unclear. We used our mouse model of arsenic-enhanced atherosclerosis to investigate the impact of the methylation process. We show that methylated arsenicals are proatherogenic, and like inorganic arsenic, alter plaque components toward a more unstable, rupture-prone phenotype. We also demonstrate that only arsenicals that undergo biotransformation are proatherogenic, supported by data showing that arsenobetaine does not increase plaque formation. Furthermore, we show that apoE$^{-/-}$ mice that also lack the enzyme that catalyzes arsenic methylation, As3MT, are protected from arsenic-, but not high-fat diet–, induced atherosclerosis. Our data also support the conclusion that arsenic biotransformation is not necessarily a detoxification process but rather is required for its proatherogenic effects.

Humans are exposed to methylated arsenicals (Oremland and Stolz 2003), but their impact on public health has been underestimated and under-evaluated. Methylated arsenicals are found in the air (Tziaras et al. 2015), soil (Mestrot et al. 2011), and water (Sánchez-Rodas et al. 2005; Schaeffer et al. 2006; Vriens et al. 2014). The relative toxicities of methylated arsenicals have been investigated *in vitro* and *in vivo*. MMA III is more cytotoxic than inorganic arsenic or DMA in cell culture systems (Stýblo et al. 2002). Similar results were observed in an endothelial cell line, where inorganic arsenic and monomethylarsonous acid diglutathione [MMA III$(GS)_2$] were more cytotoxic than MMA V and DMA V (Hirano et al. 2004). MMA III and inorganic arsenic inhibit differentiation of embryonic stem cells to the same degree, whereas DMA III has reduced effects (McCoy et al. 2015). *In vivo*, methylated arsenicals can cause hyperplasia in urothelial cells (Dodmane et al. 2013). Specifically, MMA III induces proliferation and tumorigenesis in a human urothelial cell line (Bredfeldt et al. 2006). DMA V–exposed rats pretreated with carcinogens developed a broad range of tumors in different organs (Yamamoto et al. 1995). To our knowledge, the present study is the first to show noncancer-related effects of low-moderate concentrations of methylated arsenicals *in vivo*.

Our data show that not only are methylated arsenicals proatherogenic but also that *As3mt* is required for the proatherogenic effects of arsenic in the apoE$^{-/-}$ model. This result suggests that alterations in As3MT function could be correlated with the risk of atherosclerosis. Several genetic polymorphisms in the *AS3MT* gene have been described in humans, some of which alter the enzymatic efficiency (Engström et al. 2007; Engström et al. 2011; Engström et al. 2013; Lindberg et al. 2007; Lindberg et al. 2008; Pierce et al. 2012). Indeed, arsenic methylation capacity, as measured by the presence of methylated arsenicals in the urine, is inversely associated with risk of developing disease, including cardiovascular disease (Chen et al. 2013b; Pierce et al. 2013). *AS3MT* SNPs are associated with atherosclerotic markers in humans, although these data were not significant after correcting for multiple comparisons (Wu et al. 2014). Our results support the hypothesis that *As3MT* is an important mediator of the

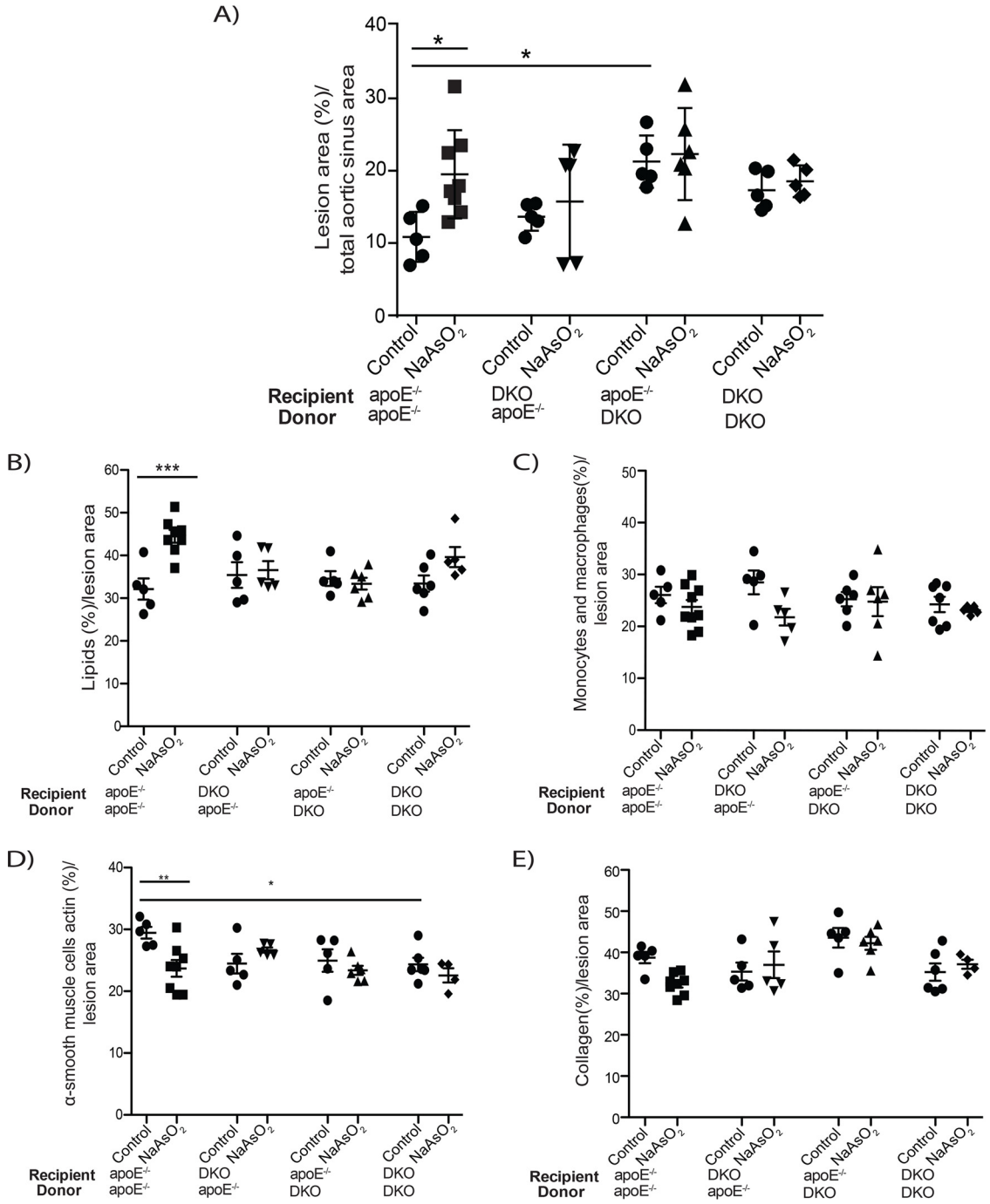

Figure 5. Effects of bone marrow–derived and non-bone marrow–derived *As3mt* on arsenic-induced atherosclerosis. Five-week-old apoE$^{-/-}$ or double knockout (DKO) male mice were lethally irradiated and transplanted as indicated. Transplanted 9-wk-old apoE$^{-/-}$ mice with apoE$^{-/-}$ bone marrow (BM), DKO mice with apoE$^{-/-}$ BM, apoE$^{-/-}$ mice with DKO BM, and DKO mice with DKO BM were exposed to 200 ppb *m*-sodium arsenite ($NaAsO_2$) for 13 wk or maintained on tap water. Sections of the aortic sinus were stained with Oil Red O, and the percentage of the lesion area was evaluated relative to the total aortic sinus area (*A*). The lipid content was evaluated relative to the total lesion area (*B*). The macrophage composition (*C*), α smooth muscle cell actin (*D*), and collagen (*E*) were also evaluated relative to the total lesion area. Values are expressed as the mean ± standard error of the mean (SEM). $^{*}p < 0.05$; $^{**}p < 0.01$; $^{***}p < 0.001$ relative to their own control.

proatherogenic effects of arsenic and should be reevaluated in multiple cohorts.

Macrophages are the main cell type that uptake and accumulate lipids at the atherosclerotic site, and they are required for generation of the atherosclerotic plaque (Ley et al. 2011; Tabas 2010). Our previous data implicated macrophages as key cellular targets in arsenic-enhanced atherosclerosis through increased lipid accumulation owing to inhibition of efflux pathways controlled by the liver X receptor (Lemaire et al. 2014; Padovani et al. 2010). We now extend these data by showing that As3MT is essential for arsenic-induced lipid accumulation in macrophages. Furthermore, our transplant studies support the concept of extrahepatic metabolism of arsenic because *As3mt* expression was required in both the hematopoietic and nonhematopoietic tissue to support the full proatherogenic effects of arsenic. Indeed, we found that As3MT is expressed and functional in several of

the key cell types in atherosclerotic plaque: macrophages, endothelial cells, and SMCs. These cell types are known to be targets of arsenic toxicity (Bourdonnay et al. 2009; Hossain et al. 2013; Lemarie et al. 2006; Lemaire et al. 2015; Lynn et al. 2000; Soucy et al. 2004; Straub et al. 2007; Straub et al. 2008; Straub et al. 2009), which leads to the intriguing possibility that arsenic methylation can occur at the site of an atherosclerotic lesion rather than only occurring in the liver with methylated arsenicals traveling to the lesion. Generation of a floxed-*As3mt* mouse is required to delineate which cells contribute to arsenic methylation in the plaque leading to atherosclerosis.

Arsenic is well known to stimulate ROS production (Straub et al. 2008; Barchowsky et al. 1996; Barchowsky et al. 1999; Nesnow et al. 2002). The extent of arsenic-induced atherosclerosis correlates with ROS within the plaques (Krohn et al. 2016). Here, we provide evidence that arsenic methylation is required for arsenic-induced ROS production *in vitro* and *in vivo*. Arsenic metabolism is required for arsenic-induced oxidative DNA damage in murine and human cell models of carcinogenicity (Kojima et al. 2009). However, the same group has shown that MMA III increases oxidative DNA damage in a methylation-deficient cell line (Orihuela et al. 2013). This finding contrasts with our data, where $NaAsO_2$ and MMA III did not induce ROS in the DKO mouse vessels and primary cells. This discrepancy could be due to the differences between primary cells, cell lines, and animals; to the apoE$^{-/-}$ background; or to the use of knockout versus poorly methylating cells. Nevertheless, our findings are intriguing and suggest that arsenic methylation is important in ROS production. Indeed, DMA III did induce ROS in cells derived from DKO mice, suggesting that this terminal metabolite may drive ROS production. Alternatively, DMA III may not be the terminal metabolite if the trimethylated form of arsenic is produced and triggers ROS production. However, this process would have to be independent of As3MT, requiring an alternate arsenic methyltransferase. ROS is one of many important factors driving atherosclerosis. Unfortunately, DMA III is too unstable to utilize in *in vivo* experiments; thus, we do not know whether DMA III would be proatherogenic in the DKO mice. Further investigation will focus on confirming DMA III–induced ROS production using multiple assays, including measures of downstream oxidative damage in the presence and absence of As3MT.

One could also hypothesize that As3MT may have other unknown functions. Although no functions have been described for As3MT beyond arsenic methylation, different metabolomic profiles have been observed in wild-type and As3mt$^{-/-}$ mice in the absence of arsenic (Huang et al. 2016). In addition, a genome-wide association study investigating the schizophrenia-associated locus linked a polymorphism in the first exon to generation of an alternatively spliced As3MT isoform, which is potentially a molecular marker for this psychiatric disease (Li et al. 2016). Given that *As3MT* lies near genes with metabolic functions on chromosome 19, perhaps deletion of exons 3–5 in the *As3MT* gene may alter the expression of nearby genes. We measured the expression of selected genes (see Table S3) upstream or downstream of *As3mt* in liver or brain of apoE$^{-/-}$ or DKO mice exposed to tap water, inorganic arsenite, or methylated arsenicals. There was variation between animals, but we found statistically significant increases in Nt5c2 mRNA in the brains of DKO mice exposed to arsenicals, and decreases in Usmg5 mRNA expression in DKO mouse livers, compared with apoE$^{-/-}$ mice (see Figure S4). Whether these changes result in similar protein changes and are functionally relevant to arsenic toxicity remains undefined.

In additional support of an alternate As3MT function, deletion of *As3mt* from apoE$^{-/-}$ mice mildly increased the basal plaque size at 17 wk of age in the aortic sinus (Figure 2), which was also observed in DKO mice transplanted with DKO bone marrow (Figure 5). A higher basal level of plaque was also observed in apoE$^{-/-}$ mice reconstituted with DKO bone marrow (Figure 5). These increases in basal plaque levels upon *As3mt* deletion were modest compared with those observed in mice fed a high-fat diet, although thus far, we have only tested mice at this relatively early time point in atherogenesis. Nevertheless, our data suggest that As3MT may protect against atherosclerosis in the absence of arsenic. Perhaps when present, arsenic quenches or sequesters As3MT, preventing antiatherogenic functions; this could explain both the increased basal plaque level upon *As3mt* deletion and the lack of arsenic-enhanced atherosclerosis in the DKO mice, even upon exposure to methylated arsenicals.

Conclusion

In summary, our data indicate a key role for *As3MT* in mediating the atherosclerotic effects of arsenic. *AS3MT* SNPs may be useful biomarkers for identifying those at greatest risk for developing cardiovascular toxicity associated with arsenic exposure.

Acknowledgments

We thank Z. Yu and S. Richard from the LDI/McGill University for technical support during antibody customization.

This work was supported by a grant from the Canadian Institutes of Health Research (MOP – 115000; to K.K.M.). L.F. N.S. was supported by a Gordon Phillips Fellowship/McGill Faculty of Medicine and by a TD Bank/LDI fellowship.

References

Ahsan H, Chen Y, Kibriya MG, Slavkovich V, Parvez F, Jasmine F, et al. 2007. Arsenic metabolism, genetic susceptibility, and risk of premalignant skin lesions in Bangladesh. Cancer Epidemiol Biomarkers Prev 16(6):1270–1278, PMID: 17548696, https://doi.org/10.1158/1055-9965.EPI-06-0676.

Andrew AS, Jewell DA, Mason RA, Whitfield ML, Moore JH, Karagas MR. 2008. Drinking-water arsenic exposure modulates gene expression in human lymphocytes from a U.S. population. Environ Health Perspect 116(4):524–531, PMID: 18414638, https://doi.org/10.1289/ehp.10861.

Argos M, Kalra T, Rathouz PJ, Chen Y, Pierce B, Parvez F, et al. 2010. Arsenic exposure from drinking water, and all-cause and chronic-disease mortalities in Bangladesh (HEALS): a prospective cohort study. Lancet 376(9737):252–258, PMID: 20646756, https://doi.org/10.1016/S0140-6736(10)60481-3.

Argos M, Parvez F, Rahman M, Rakibuz-Zaman M, Ahmed A, Hore SK, et al. 2014. Arsenic and lung disease mortality in Bangladeshi adults. Epidemiology 25(4):536–543, PMID: 24802365, https://doi.org/10.1097/EDE.0000000000000106.

ATSDR (Agency for Toxic Substances and Disease Registry). 2013. Prority list of hazardous substances. https://www.atsdr.cdc.gov/spl/ [accessed 23 September 2015].

Barchowsky A, Dudek EJ, Treadwell MD, Wetterhahn KE. 1996. Arsenic induces oxidant stress and NF-KB activation in cultured aortic endothelial cells. Free Radic Biol Medic 21(6):783–790, https://doi.org/10.1016/0891-5849(96)00174-8.

Barchowsky A, Klei LR, Dudek EJ, Swartz HM, James PE. 1999. Stimulation of reactive oxygen, but not reactive nitrogen species, in vascular endothelial cells exposed to low levels of arsenite. Free Radic Biol Med 27(11–12):1405–1412, PMID: 10641735, https://doi.org/10.1016/S0891-5849(99)00186-0.

Bourdonnay E, Morzadec C, Fardel O, Vernhet L. 2009. Redox-sensitive regulation of gene expression in human primary macrophages exposed to inorganic arsenic. J Cell Biochem 107(3):537–547, PMID: 19350554, https://doi.org/10.1002/jcb.22155.

Bredfeldt TG, Jagadish B, Eblin KE, Mash EA, Gandolfi AJ. 2006. Monomethylarsonous acid induces transformation of human bladder cells. Toxicol Appl Pharmacol 216(1):69–79, PMID: 16806342, https://doi.org/10.1016/j.taap.2006.04.011.

Bunderson M, Brooks DM, Walker DL, Rosenfeld ME, Coffin JD, Beall HD. 2004. Arsenic exposure exacerbates atherosclerotic plaque formation and increases nitrotyrosine and leukotriene biosynthesis. Toxicol Appl Pharmacol 201(1):32–39, PMID: 15519606, https://doi.org/10.1016/j.taap.2004.04.008.

Challenger F. 1947. Biological methylation. Sci Prog 35(139):396–416, PMID: 20256237.

Chen Y, Wu F, Graziano JH, Parvez F, Liu M, Paul RR, et al. 2013a. Arsenic exposure from drinking water, arsenic methylation capacity, and carotid intima-media

thickness in Bangladesh. Am J Epidemiol 178(3):372–381, PMID: 23788675, https://doi.org/10.1093/aje/kwt001.
Chen Y, Wu F, Liu M, Parvez F, Slavkovich V, Eunus M, et al. 2013b. A prospective study of arsenic exposure, arsenic methylation capacity, and risk of cardiovascular disease in Bangladesh. Environ Health Perspect 121(7):832–838, PMID: 23665672, https://doi.org/10.1289/ehp.1205797.
Chinetti-Gbaguidi G, Colin S, Staels B. 2015. Macrophage subsets in atherosclerosis. Nat Rev Cardiol 12(1):10–17, PMID: 25367649, https://doi.org/10.1038/nrcardio.2014.173.
Dangleben NL, Skibola CF, Smith MT. 2013. Arsenic immunotoxicity: a review. Environ health 12(1):73, PMID: 24004508, https://doi.org/10.1186/1476-069X-12-73.
Dheeman DS, Packianathan C, Pillai JK, Rosen BP. 2014. Pathway of human As3MT arsenic methylation. Chem Res Toxicol 27(11):1979–1989, PMID: 25325836, https://doi.org/10.1021/tx500313k.
Dodmane PR, Arnold LL, Pennington KL, Thomas DJ, Cohen SM. 2013. Effect of dietary treatment with dimethylarsinous acid (DMA (III)) on the urinary bladder epithelium of arsenic (+3 oxidation state) methyltransferase (As3MT) knockout and C57BL/6 wild type female mice. Toxicology 305:130–135, PMID: 23376817, https://doi.org/10.1016/j.tox.2013.01.015.
Drobna Z, Naranmandura H, Kubachka KM, Edwards BC, Herbin-Davis K, Styblo M, et al. 2009. Disruption of the arsenic (+3 oxidation state) methyltransferase gene in the mouse alters the phenotype for methylation of arsenic and affects distribution and retention of orally administered arsenate. Chem Res Toxicol 22(10):1713–1720, PMID: 19691357, https://doi.org/10.1021/tx900179r.
Engström K, Broberg K, Concha G, Nermell B, Warholm M, Vahter M. 2007. Genetic polymorphisms influencing arsenic metabolism: evidence from Argentina. Environ Health Perspect 115(4):599–605, PMID: 17450230, https://doi.org/10.1289/ehp.9734.
Engström K, Hossain MB, Lauss M, Ahmed S, Raqib R, Vahter M et al. 2013. Efficient arsenic metabolism—the *As3MT* haplotype is associated with DNA methylation and expression of multiple genes around *As3MT*. PLoS One 8(1): e5372, PMID: 23341986, https://doi.org/10.1371/journal.pone.0053732.
Engström K, Vahter M, Mlakar SJ, Concha G, Nermell B, Raqib R, et al. 2011. Polymorphisms in arsenic(+III oxidation state) methyltransferase (As3MT) predict gene expression of As3MT as well as arsenic metabolism. Environ Health Perspect 119(2):182–188, PMID: 21247820, https://doi.org/10.1289/ehp.1002471.
Garnier N, Redstone GG, Dahabieh MS, Nichol JN, del Rincon SV, Gu Y, et al. 2014. The novel arsenical darinaparsin is transported by cystine importing systems. Mol Pharmacol 85(4):576–585, PMID: 24431147, https://doi.org/10.1124/mol.113.089433.
Gomez D, Owens GK. 2012. Smooth muscle cell phenotypic switching in atherosclerosis. Cardiovasc Res 95(2):156–164, PMID: 22406749, https://doi.org/10.1093/cvr/cvs115.
Gu Y. 2014. Facile exchange of arsenic between adducts and implications to drug discovery [Master thesis]. Montreal, Québec:McGill University. URL: http://digitool.Library.McGill.CA:80/R/-?func=dbin-jump-full&object_id=132660&silo_library=GEN01 [accessed 6 May 2016].
Hayakawa T, Kobayashi Y, Cui X, Hirano S. 2005. A new metabolic pathway of arsenite: arsenic-glutathione complexes are substrates for human arsenic methyltransferase Cyt19. Arch Toxicol 79(4):183–191, PMID: 15526190, https://doi.org/10.1007/s00204-004-0620-x.
Hirano S, Kobayashi Y, Cui X, Kanno S, Hayakawa T, Shraim A. 2004. The accumulation and toxicity of methylated arsenicals in endothelial cells: important roles of thiol compounds. Toxicol Appl Pharmacol 198(3):458–467, PMID: 15276427, https://doi.org/10.1016/j.taap.2003.10.023.
Hossain E, Ota A, Karnan S, Damdindorj L, Takahashi M, Konishi Y, et al. 2013. Arsenic augments the uptake of oxidized ldl by upregulating the expression of lectin-like oxidized LDL receptor in mouse aortic endothelial cells. Toxicol Appl Pharmacol 273:651–658, PMID: 24145059, https://doi.org/10.1016/j.taap.2013.10.012.
Huang MC, Douillet C, Su M, Zhou K, Wu T, Chen W, et al. 2016. Metabolomic profiles of arsenic (+3 oxidation state) methyltransferase knockout mice: effect of sex and arsenic exposure. Arch Toxicol, 91(1):189–202, PMID: 26883664, https://doi.org/10.1007/s00204-016-1676-0.
Josyula AB, Poplin GS, Kurzius-Spencer M, McClellen HE, Kopplin MJ, Stürup S, et al. 2006. Environmental arsenic exposure and sputum metalloproteinase concentrations. Environ Res 102(3):283–290, PMID: 16487958, https://doi.org/10.1016/j.envres.2006.01.003.
Kojima C, Ramirez DC, Tokar EJ, Himeno S, Drobná Z, Stýblo M, et al. 2009. Requirement of arsenic biomethylation for oxidative DNA damage. J Natl Cancer Inst 101(24):1670–1681, PMID: 19933942, https://doi.org/10.1093/jnci/djp414.
Krohn RM, Lemaire M, Negro Silva LF, Lemarié C, Bolt A, Mann KK, et al. 2016. High-selenium lentil diet protects against arsenic-induced atherosclerosis in a mouse model. J Nutr Biochem 27:9–15, PMID: 26500064, https://doi.org/10.1016/j.jnutbio.2015.07.003.
Lemaire M, Lemarié CA, Flores Molina M, Guilbert C, Lehoux S, Mann KK. 2014. Genetic deletion of LXRα prevents arsenic-enhanced atherosclerosis, but not arsenic-altered plaque composition. Toxicol Sci 142(2):477–488, PMID: 25273567, https://doi.org/10.1093/toxsci/kfu197.
Lemaire M, Lemarié CA, Molina MF, Schiffrin EL, Lehoux S, Mann KK. 2011. Exposure to moderate arsenic concentrations increases atherosclerosis in apoE$^{-/-}$ mouse model. Toxicol Sci 122(1):211–221, PMID: 21512104, https://doi.org/10.1093/toxsci/kfr097.
Lemaire M, Negro Silva LF, Lemarié CA, Bolt AM, Flores Molina M, Krohn RM, et al. 2015. Arsenic exposure increases monocyte adhesion to the vascular endothelium, a pro-atherogenic mechanism. PloS One 10(9):e0136592, PMID: 26332580, https://doi.org/10.1371/journal.pone.0136592.
Lemarie A, Morzadec C, Bourdonnay E, Fardel O, Vernhet L. 2006. Human macrophages constitute targets for immunotoxic inorganic arsenic. J Immunol 177(5):3019–3027, PMID: 16920938, https://doi.org/10.4049/jimmunol.177.5.3019.
Ley K, Miller YI, Hedrick CC. 2011. Monocyte and macrophage dynamics during atherogenesis. Arterioscler Thromb Vasc Biol 31(7):1506–1516, PMID: 21677293, https://doi.org/10.1161/ATVBAHA.110.221127.
Li M, Jaffe AE, Straub RE, Tao R, Shin JH, Wang Y, et al. 2016. A human-specific *As3MT* isoform and *BORCS7* are molecular risk factors in the 10q24.32 schizophrenia-associated locus. Nat Med 22(6):649–656, PMID: 27158905, https://doi.org/10.1038/nm.4096.
Libby P, Ridker PM, Hansson GK. 2011. Progress and challenges in translating the biology of atherosclerosis. Nature 473(7347):317–325, PMID: 21593864, https://doi.org/10.1038/nature10146.
Lindberg AL, Ekström EC, Nermell B, Rahman M, Lönnerdal B, Persson LA, et al. 2008. Gender and age differences in the metabolism of inorganic arsenic in a highly exposed population in Bangladesh. Environ Res 106(1):110–120, PMID: 17900557, https://doi.org/10.1016/j.envres.2007.08.011.
Lindberg AL, Kumar R, Goessler W, Thirumaran R, Gurzau E, Koppova K, et al. 2007. Metabolism of low-dose inorganic arsenic in a central European population: Influence of sex and genetic polymorphisms. Environ Health Perspect 115(7):1081–1086, PMID: 17637926, https://doi.org/10.1289/ehp.10026.
Lynn S, Gurr JR, Lai HT, Jan KY. 2000. NADH oxidase activation is involved in arsenite-induced oxidative DNA damage in human vascular smooth muscle cells. Circ Res 86(5):514–519, PMID: 10720412, https://doi.org/10.1161/01.RES.86.5.514.
Mazumder DN. 2005. Effect of chronic intake of arsenic-contaminated water on liver. Toxicol Appl Pharmacol 206(2):169–175, PMID: 15967205, https://doi.org/10.1016/j.taap.2004.08.025.
McCoy CR, Stadelman BS, Brumaghim JL, Liu JT, Bain LJ. 2015. Arsenic and its methylated metabolites inhibit the differentiation of neural plate border specifier cells. Chem Res Toxicol 28(7):1409–1421, PMID: 26024302, https://doi.org/10.1021/acs.chemrestox.5b00036.
Mestrot A, Feldmann J, Krupp EM, Hossain MS, Roman-Ross G, Meharg AA. 2011. Field fluxes and speciation of arsines emanating from soils. Environ Sci Technol 45(5):1798–1804, PMID: 21284382, https://doi.org/10.1021/es103463d.
Molin M, Ulven SM, Meltzer HM, Alexander J. 2015. Arsenic in the human food chain, biotransformation and toxicology- review focusing on seafood arsenic. J Trace Elem Med Biol 31:249–259, PMID: 25666158, https://doi.org/10.1016/j.jtemb.2015.01.010.
Moon KA, Guallar E, Umans JG, Devereux RB, Best LG, Francesconi KA, et al. 2013. Association between exposure to low to moderate arsenic levels and incident cardiovascular disease. A prospective cohort study. Ann Intern Med 159(10):649–659, PMID: 24061511, https://doi.org/10.7326/0003-4819-159-10-201311190-00719.
Navas-Acien A, Francesconi KA, Silbergeld EK, Guallar E. 2011. Seafood intake and urine concentrations of total arsenic, dimethylarsinate and arsenobetaine in the us population. Environ Res 111(1):110–118, PMID: 21093857, https://doi.org/10.1016/j.envres.2010.10.009.
Navas-Acien A, Silbergeld EK, Pastor-Barriuso R, Guallar E. 2008. Arsenic exposure and prevalence of type 2 diabetes in US adults. JAMA 300(7):814–822, PMID: 18714061, https://doi.org/10.1001/jama.300.7.814.
Nesnow S, Roop BC, Lambert G, Kadiiska M, Mason RP, Cullen WR, et al. 2002. DNA damage induced by methylated trivalent arsenicals is mediated by reactive oxygen species. Chem Res Toxicol 15(12):1627–1634, PMID: 12482246, https://doi.org/10.1021/tx025598y.
Nordstrom DK. 2002. Public health. Worldwide occurrences of arsenic in ground water. Science 296(5576):2143–2145, PMID: 12077387, https://doi.org/10.1126/science.1072375.
Oremland RS, Stolz JF. 2003. The ecology of arsenic. Science 300(5621):939–944, PMID: 12738852, https://doi.org/10.1126/science.1081903.
Orihuela R, Kojima C, Tokar EJ, Person RJ, Xu Y, Qu W, et al. 2013. Oxidative DNA damage after acute exposure to arsenite and monomethylarsonous acid in biomethylation-deficient human cells. Toxicol Mech Methods 23(6):389–395, PMID: 23301828, https://doi.org/10.3109/15376516.2012.762570.

Padovani AM, Molina MF, Mann KK. 2010. Inhibition of liver X receptor/retinoid X receptor-mediated transcription contributes to the proatherogenic effects of arsenic in macrophages in vitro. Arterioscler Thromb Vasc Biol 30(6):1228–1236, PMID: 20339114, https://doi.org/10.1161/ATVBAHA.110.205500.

Pierce BL, Kibriya MG, Tong L, Jasmine F, Argos M, Roy S, et al. 2012. Genome-wide association study identifies chromosome 10q24.32 variants associated with arsenic metabolism and toxicity phenotypes in Bangladesh. PLoS Genet 8(2):e1002522, PMID: 22383894, https://doi.org/10.1371/journal.pgen.1002522.

Pierce BL, Tong L, Argos M, Gao J, Farzana J, Roy S, et al. 2013. Arsenic metabolism efficiency has a causal role in arsenic toxicity: Mendelian randomization and gene-environment interaction. Intern J Epidemiol 42(6):1862–1871, PMID: 24536095, https://doi.org/10.1093/ije/dyt182.

Ray JL, Leach R, Herbert JM, Benson M. 2001. Isolation of vascular smooth muscle cells from a single murine aorta. Methods Cell Sci 23(4):185–188, PMID: 12486328, https://doi.org/10.1023/A:1016357510143.

Robins RS, Lemarié CA, Laurance S, Aghourian MN, Wu J, Blostein MD. 2013. Vascular Gas6 contributes to thrombogenesis and promotes tissue factor up-regulation after vessel injury in mice. Blood 121(4):692–699, PMID: 23149844, https://doi.org/10.1182/blood-2012-05-433730.

Sánchez-Rodas D, Luis Gómez-Ariza J, Giráldez I, Velasco A, Morales E. 2005. Arsenic speciation in river and estuarine waters from southwest Spain. Sci Total Environ 345(1–3):207–217, PMID: 15919540, https://doi.org/10.1016/j.scitotenv.2004.10.029.

Schaeffer R, Francesconi KA, Kienzl N, Soeroes C, Fodor P, Váradi L, et al. 2006. Arsenic speciation in freshwater organisms from the river Danube in Hungary. Talanta 69(4):856–865, PMID: 18970648, https://doi.org/10.1016/j.talanta.2005.11.025.

Smith AH, Marshall G, Liaw J, Yuan Y, Ferreccio C, Steinmaus C. 2012. Mortality in young adults following in utero and childhood exposure to arsenic in drinking water. Environ Health Perspect 120(11):1527–1531, PMID: 22949133, https://doi.org/10.1289/ehp.1104867.

Soucy NV, Klei LR, Mayka DD, Barchowsky A. 2004. Signaling pathways for arsenic-stimulated vascular endothelial growth factor-a expression in primary vascular smooth muscle cells. Chem Res Toxicol 17(4):555–563, PMID: 15089098, https://doi.org/10.1021/tx034193q.

Straub AC, Clark KA, Ross MA, Chandra AG, Li S, Gao X, et al. 2008. Arsenic-stimulated liver sinusoidal capillarization in mice requires nadph oxidase-generated superoxide. J Clin Invest 118(12):3980–3989, PMID: 19033667, https://doi.org/10.1172/JCI35092.

Straub AC, Klei LR, Stolz DB, Barchowsky A. 2009. Arsenic requires sphingosine-1-phosphate type 1 receptors to induce angiogenic genes and endothelial cell remodeling. Am J Pathol 174(5):1949–1958, PMID: 19349368, https://doi.org/10.2353/ajpath.2009.081016.

Straub AC, Stolz DB, Ross MA, Hernández-Zavala A, Soucy NV, Klei LR, et al. 2007. Arsenic stimulates sinusoidal endothelial cell capillarization and vessel remodeling in mouse liver. Hepatology 45(1):205–212, PMID: 17187425, https://doi.org/10.1002/hep.21444.

Stýblo M, Drobná Z, Jaspers I, Lin S, Thomas DJ. 2002. The role of biomethylation in toxicity and carcinogenicity of arsenic: a research update. Environ Health Perspect 110(suppl 5):767–771, PMID: 12426129, http://www.jstor.org/stable/3455089.

Tabas I. 2010. Macrophage death and defective inflammation resolution in atherosclerosis. Nat Rev Immunol 10(1):36–46, PMID: 19960040, https://doi.org/10.1038/nri2675.

Thomas DJ, Li J, Waters SB, Xing W, Adair BM, Drobna Z, et al. 2007. Arsenic (+3 oxidation state) methyltransferase and the methylation of arsenicals. Exp Biol Med (Maywood) 232(1):3–13, PMID: 17202581.

Tokar EJ, Diwan BA, Ward JM, Delker DA, Waalkes MP. 2011. Carcinogenic effects of "whole-life" exposure to inorganic arsenic in CD1 mice. Toxicol Sci 119(1):73–83, PMID: 20937726, https://doi.org/10.1093/toxsci/kfq315.

Tziaras T, Pergantis SA, Stephanou EG. 2015. Investigating the occurrence and environmental significance of methylated arsenic species in atmospheric particles by overcoming analytical method limitations. Environ Sci Technol 49(19):11640–11648, PMID: 26335501, https://doi.org/10.1021/acs.est.5b02328.

Vahter M, Marafante E, Dencker L. 1983. Metabolism of arsenobetaine in mice, rats and rabbits. Sci Total Environ 30:197–211, PMID: 6648507, https://doi.org/10.1016/0048-9697(83)90012-8.

Vriens B, Ammann AA, Hagendorfer H, Lenz M, Berg M, Winkel LH. 2014. Quantification of methylated selenium, sulfur, and arsenic in the environment. PloS One 9(7):e102906, PMID: 25047128, https://doi.org/10.1371/journal.pone.0102906.

WHO (World Health Organization). 2001. United Nations synthesis report on arsenic in drinking water. https://www.ircwash.org/sites/default/files/UNACC_2001-United.pdf [accessed 12 June 2017].

Wu F, Jasmine F, Kibriya MG, Liu M, Cheng X, Parvez F, et al. 2014. Interaction between arsenic exposure from drinking water and genetic susceptibility in carotid intima-media thickness in Bangladesh. Toxicol Appl Pharmacol 276(3):195–203, PMID: 24593923, https://doi.org/10.1016/j.taap.2014.02.014.

Yamamoto S, Konishi Y, Matsuda T, Murai T, Shibata MA, Matsui-Yuasa I, et al. 1995. Cancer induction by an organic arsenic compound, dimethylarsinic acid (cacodylic acid), in F344/DuCrj rats after pretreatment with five carcinogens. Cancer Res 55(6):1271–1276, PMID: 7882321, http://cancerres.aacrjournals.org/content/55/6/1271.